Periodically pulsed laser-assisted tunneling may generate terahertz radiation

Mark J. Hagmann, Dmtrij G. Coombs, and Dmitry A. Yarotski

Citation: Journal of Vacuum Science & Technology B **35**, 03D109 (2017); doi: 10.1116/1.4979549
View online: https://doi.org/10.1116/1.4979549
View Table of Contents: http://avs.scitation.org/toc/jvb/35/3
Published by the American Vacuum Society

Periodically pulsed laser-assisted tunneling may generate terahertz radiation

Mark J. Hagmann[a] and Dmtrij G. Coombs[b]
NewPath Research L.L.C., 2880 S. Main St., Suite. 214, Salt Lake City, Utah 84115

Dmitry A. Yarotski
Center for Integrated Nanotechnologies, Materials Physics and Applications Division, Los Alamos National Laboratory, Los Alamos, New Mexico 87545

(Received 14 January 2017; accepted 17 March 2017; published 24 April 2017)

A mode-locked ultrafast laser focused on the tunneling junction of a scanning tunneling microscope superimposes harmonics of the laser pulse repetition frequency on the direct current tunneling current. The power measured at the first 200 harmonics (up to 14.85 GHz) varies as the inverse square of the frequency due to shunting by the stray capacitance and the resistance in the circuit. However, Fourier analysis suggests that within the tunneling junction there is no significant decay of the harmonics until terahertz frequencies comparable to the reciprocal of the laser pulse-width. Two different types of analysis are used to model the generation of the frequency comb within the tunneling junction. Similar results are obtained, suggesting that the harmonics may extend to terahertz frequencies. Thus, the tunneling junction may be used as a subnanometer sized source of terahertz radiation. © *2017 American Vacuum Society*. [http://dx.doi.org/10.1116/1.4979549]

I. INTRODUCTION

A mode-locked ultrafast laser superimposes hundreds of harmonics of the pulse repetition frequency (PRF) on the direct current (DC) tunneling current in a tunneling junction as a microwave frequency comb (MFC). Measurements with a scanning tunneling microscope (STM) show the full-width-half-maximum (FWHM) linewidth of each harmonic is less than 0.1 Hz, so the quality factor Q is greater than 10^{11} at the 200th harmonic (14.85 GHz).[1] However, the power at the first 200 harmonics varies approximately as the inverse square of the frequency due to shunting by stray capacitance and the resistance in the circuit. Now analysis is used to determine the spectrum of the current source of the MFC via optical rectification within the tunneling junction. This work is an extension of our earlier measurements of the MFC when mode-locked ultrafast lasers are used to generate terahertz radiation by electron-hole pair creation in semiconductors[2] and optical rectification in ZnTe.[3] Previous pioneering work by Krieger[4] and group used CW lasers for optical heterodyning and subsequently determined that the effect they saw was primarily thermal. By contrast, we are using a mode-locked ultrafast laser and measure harmonics of the laser PRF. The only decay that we see in these harmonics in measurement, external to the tunneling junction, is explainable by the shunting of the signal by parasitic capacitance. Thus, perhaps due to the extremely low duty cycle of our laser, we do not see a thermal effect.

II. MEASUREMENTS OF THE MFC

We have measured the MFC by using a passively mode-locked Ti:sapphire laser, a STM, and a spectrum analyzer for detection.[1] The laser has a PRF of 74.254 MHz corresponding to $T = 13.47$ ns, a pulse width $\tau \approx 15$ fs, and a timing jitter with $\delta \approx 100$ fs. Current division between the spectrum analyzer load resistance $R_L = 50\,\Omega$ and the stray capacitance $C_S = 6.4$ pF causes the measured power at the kth harmonic (k/T) to vary as in 1 where P_1 is the measured power at the fundamental $(k = 1)$. Note that for large k the measured power varies approximately as the inverse square of the harmonic number

$$P_k = \frac{1 + \left(2\pi \frac{R_L C_S}{T}\right)^2}{1 + \left(2\pi k \frac{R_L C_S}{T}\right)^2} P_1. \quad (1)$$

The frequency of the fundamental is low enough that the effects of R_L and C_S in the measurement circuit are negligible. Thus, we assume that an RMS current of 3.99 nA, corresponding to the measured power of −121 dBm at the fundamental in the MFC, is a good approximation of the current at the fundamental within the tunneling junction.

III. ANALYSIS BASED ON OPTICAL RECTIFICATION

The tunneling junction is much smaller than the laser wavelength. Thus, we previously used the measured DC current–voltage relationship to approximate the effect of optical rectification. Therefore, focusing a mode-locked ultrafast laser on a tunneling junction creates a regular sequence of current pulses having a waveform similar to the envelope for the laser radiation. Fourier analysis shows that within the tunneling junction the spectrum would be a frequency comb of harmonics having comparable amplitude until the frequency is comparable with $2/\tau$, where τ is the pulse-width for the laser. Furthermore, the linewidth would approach zero in the ideal limit of perfect periodicity in the laser radiation.

[a]Present address: Department of Electrical and Computer Engineering, The University Of Utah, Salt Lake City, Utah 84115; electronic mail: newpathresearch@gmail.com
[b]Present address: Department of Mathematics, The University of Utah, Salt Lake City, Utah 84112.

We previously derived an expression for the power spectral density (PSD) of the frequency comb[1] [Eq. (7) of Ref. 1]

$$G(\omega) = \frac{I_0^2 R\tau^2}{(2N+1)T} e^{-\left(\omega^2\tau^2/4\right)} \times \sum_{n=-N}^{N} e^{i\omega(nT-\Theta_n)} \sum_{m=-N}^{N} e^{i\omega(mT-\Theta_m)}. \quad (2)$$

Here, ω is the frequency, τ is the laser pulse-width, T is the ideal time between consecutive laser pulses, and R is the resistance seen by the regular sequence of current pulses. In deriving Eq. (2), we allow for the effects of the envelope coherence length $L = (2N+1)T$ and timing jitter where the random variable Θ_n, the offset of the nth current pulse, is assumed to have a probability density of $1/\delta$ over the interval $(-\delta/2, \delta/2)$.

At the resonant frequencies given by $f_k = k/T$ the PSD is given by

$$G_k = \frac{I_0^2 R\tau^2}{(2N+1)T} e^{-\pi^2 k^2 (\tau/T)^2} \times \sum_{n=-N}^{N} e^{i\omega(nT-\Theta_n)} \sum_{m=-N}^{N} e^{-i\omega(mT-\Theta_m)}. \quad (3)$$

For the special case of no timing jitter

$$G_k = (2N+1)\frac{I_0^2 R\tau^2}{T} e^{-\pi^2 k^2 (\tau/T)^2}. \quad (4)$$

Half-way between each pair of resonances the frequencies are given by $f_h = (k+1/2)/T$. There is a negligible change in the exponential so the from Eq. (3) gives the following expression for the PSD:

$$G_k = \frac{I_0^2 R}{(2N+1)} \left(\frac{\tau^2}{T}\right) e^{-\pi^2 k^2 (\tau/T)^2} \times \sum_{n=-N}^{N} (-1)^n e^{i\left(((2k+1)\pi)/T\right)\Theta_n} \times \sum_{m=-N}^{N} (-1)^m e^{-i\left(((2k+1)\pi)/T\right)\Theta_m}. \quad (5)$$

Partial cancellation of the terms in the product of the two summations in Eq. (5) causes the PSD to be much lower half-way between each adjacent pair of the resonances. For the special case where the timing jitter may be neglected, Eq. (5) simplifies to Eq. (6), and the ratio G_h/G_k is given by Eq. (7) showing that $G_h \ll G_k$ because N is large,

$$G_h = \frac{I_0^2 R\tau^2}{(2N+1)T} e^{-\pi^2 k^2 (\tau/T)^2}, \quad (6)$$

$$\frac{G_h}{G_k} = \frac{1}{(2N+1)^2}. \quad (7)$$

Next we consider the PSD at a small displacement from the resonance such that $f_\epsilon = (k+\epsilon)/T$

$$G_{k\epsilon} = \frac{I_0^2 R\tau^2}{(2N+1)T} e^{-\pi^2 k^2 (\tau/T)^2} \times \sum_{n=-N}^{N} e^{-i\left(n\epsilon-(k+\epsilon)(\Theta_n/T)\right)} \times \sum_{m=-N}^{N} e^{i\left(m\epsilon-(k+\epsilon)(\Theta_m/T)\right)}. \quad (8)$$

The parameter k is a nonzero integer and we require $\epsilon \ll 1$ so Eq. (8) may be simplified as follows:

$$G_{k\epsilon} = \frac{I_0^2 R\tau^2}{(2N+1)T} e^{-\pi^2 k^2 (\tau/T)^2} \times \sum_{n=-N}^{N} e^{-i(n\epsilon-k(\Theta_n/T))} \sum_{m=-N}^{N} e^{i(m\epsilon-k(\Theta_m/T))}. \quad (9)$$

For the special case where the timing jitter may be neglected, Eq. (9) simplifies to Eq. (11). The product of the two summations is taken in Eq. (11) and is simplified to obtain Eq. (12)

$$G_{k\epsilon} = \frac{I_0^2 R\tau^2}{(2N+1)T} e^{-\pi^2 k^2 (\tau/T)^2} \times \sum_{n=-N}^{N} e^{-in\epsilon} \sum_{m=-N}^{N} e^{im\epsilon}, \quad (10)$$

$$G_{k\epsilon} = \frac{I_0^2 R\tau^2}{(2N+1)T} e^{-\pi^2 k^2 (\tau/T)^2} \times (1 + 2\cos\epsilon + 2\cos 2\epsilon + \ldots + 2\cos N\epsilon)^2, \quad (11)$$

$$G_{k\epsilon} = \frac{I_0^2 R\tau^2}{(2N+1)T} e^{-\pi^2 k^2 (\tau/T)^2} \times \left(1 + \frac{2\sin\frac{N\epsilon}{2}\cos\frac{(N+1)\epsilon}{2}}{\sin\frac{\epsilon}{2}}\right)^2. \quad (12)$$

For graphics, it is useful to define the normalized PSD, $G_{k\epsilon N}$, in Eq. (13) where an expression for $G_{k\epsilon N}$ is given in Eq. (14). Figure 1 shows this variable as a function of ϵ for any value of k where the resonant frequency $f_k = k/T$ and the displacement from the resonant frequency is ϵ/T. Thus, at this level of approximation, within the tunneling junction the linewidth is the same for each resonance. Figure 1 also shows that at each resonant frequency the normalized PSD is equal to $2N+1$, which is readily seen in the limit as ϵ approaches zero in Eq. (14)

$$G_{k\epsilon N} = \frac{T}{I_0^2 R\tau^2} e^{\pi^2 k^2 (\tau/T)^2} G_{k\epsilon}, \quad (13)$$

$$G_{k\epsilon N} = \frac{1}{2N+1}\left(1 + \frac{2\sin\frac{N\epsilon}{2}\cos\frac{(N+1)\epsilon}{2}}{\sin\frac{\epsilon}{2}}\right)^2. \quad (14)$$

Equation (15) is obtained by setting $G_{k\epsilon N} = 1/2$ with $N \gg 1$ and $\epsilon \ll 1$, and solved in Eqs. (16) and (17) to determine ϵ as a function of N at the 3-dB points

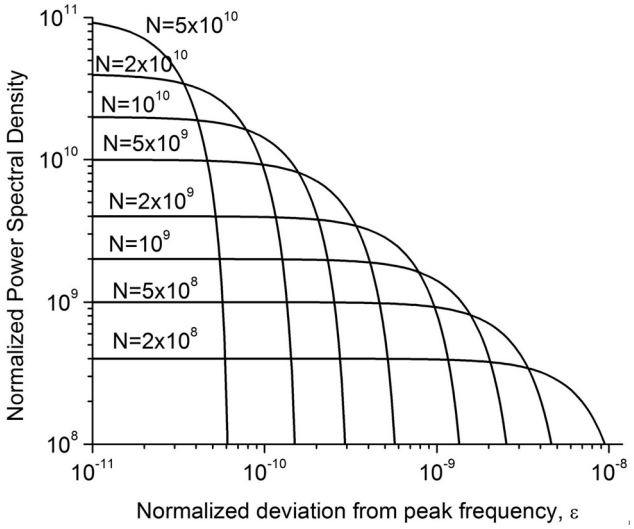

FIG. 1. Normalized PSD $G_{k\epsilon N}$, vs ϵ for different values of N in Eq. (12).

$$\left(1+\frac{2\sin\frac{N\epsilon}{2}\cos\frac{N\epsilon}{2}}{\frac{\epsilon}{2}}\right)^2=N, \tag{15}$$

$$\left(\frac{1}{N}+\frac{2\sin N\epsilon}{N\epsilon}\right)^2=\frac{1}{N}, \tag{16}$$

$$\epsilon=\pm\frac{\pi}{N}. \tag{17}$$

Thus, the FWHM linewidth is given by $2\pi/NT$. This expression has been verified using the data for 1 as well as other cases in which $N\gg 1$ and $\epsilon\ll 1$. Now, using this result with Eq. (4) we obtain the following approximation for the power at the kth harmonic:

$$P_k=4\pi I_0^2R\left(\frac{\tau}{T}\right)^2e^{-\pi^2k^2(\tau/T)^2}. \tag{18}$$

Thus, the RMS value of the current at the k*th* harmonic within the tunneling junction is given by

$$I_{\mathrm{RMSk}}=\sqrt{8\pi}I_0\frac{\tau}{T}e^{-\left(\pi^2k^2/2\right)(\tau/T)^2}. \tag{19}$$

The MFC has unique properties, as described in the Introduction, but now we address the phenomena within the tunneling junction. For example, the exponential term in Eq. (2) suggests that within the tunneling junction the 3-dB point is at $k=2.4\times10^5$ corresponding to 18 THz. As noted earlier, we assume that an RMS current of 3.99 nA, corresponding to the measured power of −121 dBm at the fundamental in the MFC, is a good approximation to the current at the fundamental within the tunneling junction. Thus, Eq. (4) shows that the parameter $I_0=1.52$ mA. Substituting the value for I_0 into Eq. (19) and approximating the summation over k, it may be shown that if all of the harmonics were to add in phase during each laser pulse, the total peak current in the tunneling junction would be approximately 2 mA. There is a power of –121 dBm in the fundamental at each of the first 2×10^5 harmonics. This corresponds to a power at each harmonic of 0.794 fW and a total power of 159 pW, most of which is at terahertz frequencies.

In measurements of the MFC, we see a FWHM linewidth of 0.1 Hz as an upper limit for the actual value that is set by the finite resolution bandwidth of the spectrum analyzer.[1] Because this value is seen even at the fundamental of the MFC where the measurement circuit does not interfere, we consider 0.1 Hz as an upper bound for the linewidth at all of the harmonics within the tunneling junction. Equation (17) shows that N must be greater than 4×10^9 to obtain a linewidth less than 0.1 Hz with our apparatus, which sets a lower bound of 100 s for the envelope coherence length of the laser. However, the derivation of Eq. (17) requires the approximation of zero timing jitter so these are lower bounds for both N and the envelope coherence length.

Figure 2 shows the RMS values for the current at each harmonic of the frequency comb, both within the tunneling junction and in the external load, calculated using Eqs. (19) and (1).

IV. ANALYSIS WITH SQUARE BARRIER MODEL

The analysis in Sec. III was based on the *ad hoc* assumption that the effects of optical rectification are well approximated with the DC current–voltage relationship. Now the Schrödinger equation is solved using a square barrier approximation model for the tunneling junction.

Consider the square-barrier approximation of a tunneling junction where a particle with energy E is incident upon a barrier with height V_0 on $x\in(0,d)$ where $d\approx0.1$ nm. The laser induced potential is modeled as $U_1(t)=V_1\cos\omega_0t$ for $t\in(-\tau/2,\tau/2)$ and zero everywhere else over a period from $t\in(-T/2,T/2)$. This allows for an attainable analytic solution that preserves the phenomena we are interested in modeling. This is consistent with similar models previously used by Büttiker and Landauer.[5] Calculating the Fourier series (Appendix), we have from Eq. (A1),

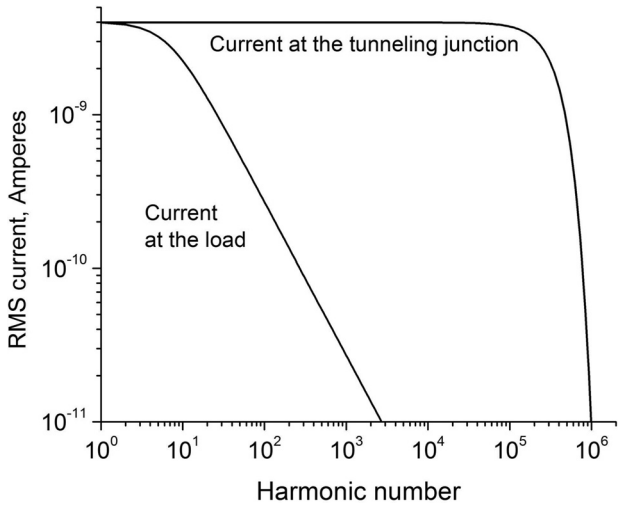

FIG. 2. Simulated RMS current at each harmonic of the frequency comb at the tunneling junction and in the load for our apparatus.

$$\Omega_{\pm} = \frac{\omega_0 \tau}{2} \pm n\pi \frac{\tau}{T}, \tag{20}$$

$$C_n = \left(\sin c(\Omega_+) + \sin c(\Omega_-)\right), \tag{21}$$

$$C_0 = \sin c\left(\frac{\omega_0 \tau}{2}\right), \tag{22}$$

$$U_1(t) = V_1 \frac{\tau}{T} C_0 + V_1 \frac{\tau}{T} \sum_{n=1}^{\infty} C_n \cos \frac{2\pi n t}{T}. \tag{23}$$

Schrödinger's equation on $x \in (0, d)$ then becomes

$$-\frac{\hbar^2}{2m} \Psi_{xx} + (V_0 + U_1(t))\Psi = i\hbar \Psi_t \,. \tag{24}$$

By Flouquet's theorem,[6] we assume a solution of the form

$$\Psi(x,t) = \sum_{p=-\infty}^{\infty} \phi_p(x) e^{-iEt/\hbar} e^{-ip\omega_T t}, \tag{25}$$

where $\omega_T = 2\pi/T$.

Substituting Eq. (25) into Eq. (24), applying Euler's theorem to $U_1(t)$, removing the sum with respect to p, noting that $\Psi_{p+n} = \Psi_p e^{-in\omega_T t}$ and simplifying yields

$$-\frac{\hbar^2}{2m}\frac{\partial^2 \Psi_p}{\partial x^2} + V_1 \frac{\tau}{T} \sum_{n=1}^{\infty} \frac{C_n}{2} (\Psi_{p-n} + \Psi_{p+n}) - \left(p\hbar\omega_T + E - V_0 - V_1 \frac{\tau}{T} C_0\right) \Psi_p = 0. \tag{26}$$

We must now make some conclusions about $\Psi_{p\pm n}$. The shift energies are created by multiphoton processes[7] of energy corresponding with the pulsed modulation of the laser. Here, $p\hbar\omega_T$ is much smaller than E as $\hbar\omega_T$ is on the order of 3×10^{-7} eV. It is very important to note that these shift energies are irrespective of the optical carrier frequency and only dependent on the PRF. Therefore, the shifts have a negligible effect on the wave function Ψ_p. We can conclude $\Psi_{p\pm n} \approx \Psi_p$ for somewhat large n. Also, we can combine terms in Eq. (26) and cancel the time dependence

$$-\frac{\hbar^2}{2m}\frac{\partial^2 \phi_p}{\partial x^2} - \left(E - V_0 - V_1 \frac{\tau}{T} C_0 - V_1 \frac{\tau}{T} \sum_{n=1}^{\infty} C_n\right) \phi_p = 0 \,. \tag{27}$$

If we now consider the sums of the sinc functions that make up C_n with the typical values previously described we generate the following graph.

Figure 3 shows the value for the coefficient C_n Eq. (21) as a function of the index n, using the parameters defined in the previous paragraph. A logarithmic scale is used in 3 to emphasize that C_n has a constant value of -0.1052 to the first $n = 10^5$ harmonics corresponding to the frequencies below 8 terahertz. Therefore, the $n = 10^5$ partial sum of C_n is $\alpha \approx 10520$. C_0 is on the order of 10^{-1} and is small relative to α, allowing us to neglect it. Thus, Eq. (27) simplifies to

$$-\frac{\hbar^2}{2m}\frac{\partial^2 \phi_p}{\partial x^2} - \left(E - V_0 - \alpha \frac{\tau}{T} V_1\right) \phi_p = 0 \,. \tag{28}$$

The solution to which is

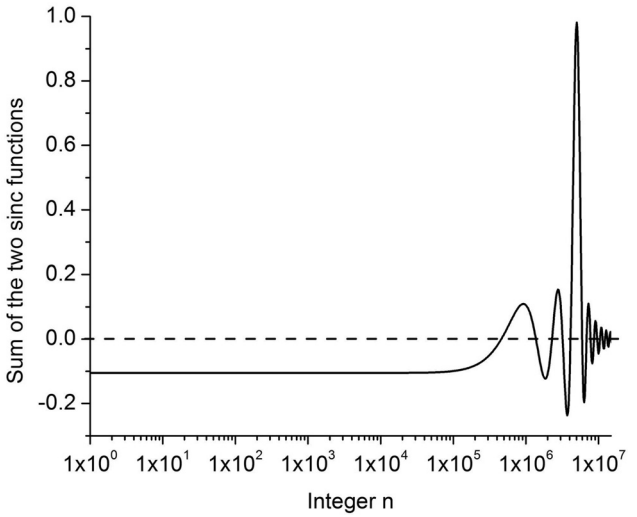

FIG. 3. Coefficient C_n vs index n (log scale).

$$\phi_p(x) = A_p e^{kx} + B_p e^{-kx}, \tag{29}$$

for $k = \sqrt{2m(E - V_0 - \alpha(\tau/T)V_1)/\hbar^2}$.

We can also conclude with our previous approximations that A_p and B_p change little with respect to p for $|p| \leq N$ (N depends on the number of possible energy shifts between E and V_0) as $\phi_p \approx \phi_{p\pm n}$. Therefore, $\Psi(x,t)$ is given by

$$\Psi(x,t) = \phi(x) e^{-iEt/\hbar} \sum_{p=-N}^{N} e^{-ip\omega_T t}, \quad \text{for} \quad \phi(x) = Ae^{kx} + Be^{-kx}. \tag{30}$$

Now we calculate the probability density current $\vec{J}$ in the positive x-direction inside the square barrier

$$\vec{J} = \frac{i\hbar}{2m} (\Psi \nabla \Psi^* - \Psi^* \nabla \Psi)\, \hat{x} \,. \tag{31}$$

Substituting Eq. (30) into Eq. (31), we obtain

$$\vec{J} = \frac{i\hbar k}{m} (AB^* - A^* B) \times \left(\sum_{p=-N}^{N} e^{-ip\omega_T t}\right) \left(\sum_{p=-N}^{N} e^{ip\omega_T t}\right) \hat{x}. \tag{32}$$

Since indexes are symmetric and functions reflexive this is equivalent to

$$\vec{J} = \frac{i\hbar k}{m} (AB^* - A^* B) \left(\sum_{p=-N}^{N} e^{ip\omega_T t}\right)^2 \hat{x} \,. \tag{33}$$

Expanding the square of the sum yields

$$\vec{J} = \frac{i\hbar k}{m} (AB^* - A^* B) \times \sum_{p=-2N}^{2N} \left((2N+1) - |p|\right) e^{ipS\omega_T t}\, \hat{x}. \tag{34}$$

By Euler's formula

$$\vec{J} = \frac{2i\hbar k}{m}(AB^* - A^*B) \times \left(\frac{(2N+1)}{2} + \sum_{p=1}^{2N}((2N+1)-p)\cos p\omega_T t\right)\hat{x}. \tag{35}$$

Due to the un-normalized nature of the series in Eq. (35), we cannot directly solve for the total current. The upper limit on usable values of N is dependent on how near the energy E is to the barrier height V_0. When these energy shifts caused by multiphoton processes become comparable to $V_0 - E$ then the energy-shifted wave functions in Eq. (26) are no longer close, increasing the spread in energies, and coupling can no longer be removed from Eq. (26). Therefore, further assumptions become unsupportable. Examining the sum in Eq. (35), $\cos p\omega_T t$ is maximum at $t = n\pi/p\omega_T$. All of these currents constructively interfere at $t = 2n\pi/\omega_T$ which corresponds to a frequency of $f_T = \omega_T/2\pi = 74.254$ MHz. This is expected as that is the PRF of our laser. What is of greater interest is the existence of frequency components of the current into the terahertz range. Equation (35) suggests that the MFC current decays linearly with respect to the harmonics p. Mathematically, Eq. (35) indicates that near to $p = 0$ the distribution of contribution to the probability density current is linearly decreasing with respect to p Eq. (4). In this model, for terahertz frequencies to have contributions to the tunneling current, we would require

$$p \geq \frac{1 \times 10^{12}}{74.254 \times 10^6} = 1.3467 \times 10^4. \tag{36}$$

In order for p to have a contribution of one-half of the fundamental $(p = 1)$, we need $p = N + 1 \approx N$. Therefore, the current at 1 THz is one-half of the current at the fundamental if $N = 1.3467 \times 10^4$ as can be seen in Eq. (4).

Now, let us approximate the energy-barrier difference that is allowed for such a N. In order for N E-shifts to be 2 orders of magnitude smaller than $V_0 - E$ to preserve our model

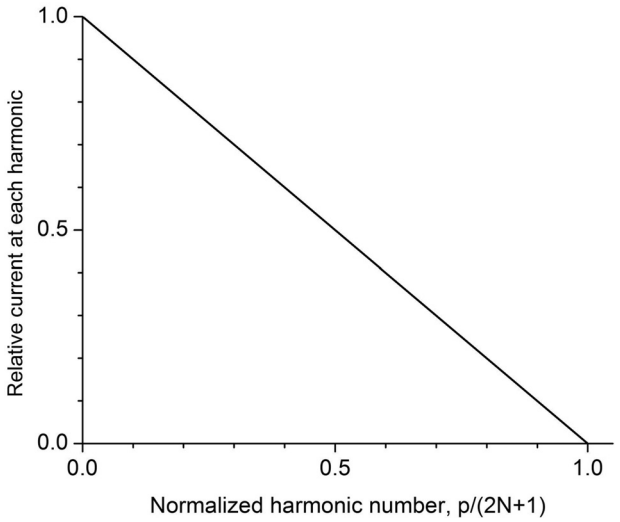

FIG. 4. Relative current contribution vs normalized harmonic number $p/2N + 1$.

$$N \approx \frac{V_0 - E}{10^2\hbar\omega_T}. \tag{37}$$

Solving for $V_0 - E$

$$(V_0 - E) \approx 10^2 N\hbar\omega_T \approx 3N \times 10^{-5}\,\text{eV}. \tag{38}$$

At $N = \approx 1.3467 \times 10^4$

$$(V_0 - E) \approx 0.404\,\text{eV}. \tag{39}$$

This shows that in order for the 1 THz component to be half that of the PRF (74.254 MHz) contribution and our model would only be accurate if $V_0 - E$ is greater than 0.404 eV. This is shown in Fig. 4, which shows the relative current contribution as a function of the normalized harmonic number.

V. CONCLUSION

Two different methods have been used to model the generation of the frequency comb. In one method, the current–voltage relationship at DC is used to predict optical rectification. In the second method, the time dependent Schrödinger equation is solved with the approximation of a square potential barrier subject to a spatially independent modulation. Both methods predict that the frequency comb extends to terahertz frequencies within the tunneling junction. The second method indicates that optical rectification is maintained until at least terahertz frequencies for sufficient energy-barrier differentials. Thus, we conclude, the tunneling junction may be used as a subnanometer sized source of terahertz radiation. Others[8] have focused a terahertz laser on a conical metal tip for local enhancement of the radiation by near-field confinement. The tip, attached to the cantilever of an atomic force microscope, was scanned across a semiconductor. This enabled the carrier concentration to be imaged with a spatial resolution of 40 nm. We conclude that it may be possible to obtain subnanometer resolution by using the terahertz radiation generated in the tunneling junction as we have described.

ACKNOWLEDGMENTS

This work was performed, in part, at the Center for Integrated Nanotechnologies, a U.S. Department of Energy, Office of Basic Energy Sciences user facility. Los Alamos National Laboratory, an affirmative action equal opportunity employer, is operated by Los Alamos National Security, LLC, for the National Nuclear Security Administration of the U.S. Department of Energy under Contract No. DE-AC52-06NA25396.

APPENDIX: FOURIER SERIES FOR LASER INDUCED TIME-DEPENDENT POTENTIAL ALLOWING FOR OPTICAL CARRIER

The laser induced electric field is modeled as $f(t) = E_1 \cos\omega_0 t$ for $t \in (-\tau/2, \tau/2)$ and zero everywhere else over a period from $t \in (-T/2, T/2)$. We approximate the induced potential as $U_1(t) = V_1 \cos\omega_0 t$ with the same conditions on the same domain. This allows for an attainable analytic solution that preserves the phenomena we are interested in modeling. The Fourier series for $U_1(t)$ is then given by[1]

$$U_1(t) = V_1 \frac{\tau}{T}\left(\frac{\sin\frac{\omega_0\tau}{2}}{\frac{\omega_0\tau}{2}}\right) + V_1\frac{\tau}{T}\sum_{n=1}^{\infty}\left(\frac{\sin\Omega_+}{\Omega_+}+\frac{\sin\Omega_-}{\Omega_-}\right)\cos\left(\frac{2\pi nt}{T}\right), \tag{A1}$$

where $\Omega_\pm = (\omega_0\tau/2)\pm n\pi(\tau/T)$.

[1]M. J. Hagmann, F. S. Stenger, and D. A. Yarotski, J. Appl. Phys. **114**, 223107 (2013).
[2]M. J. Hagmann, S. Pandey, A. Nahata, A. J. Taylor, and D. A. Yarotski, Appl. Phys. Lett. **101**, 231102 (2012).
[3]M. J. Hagmann, T. E. Henage, A. K. Azad, A. J. Taylor, and D. A. Yarotski, Electron. Lett. **49**, 1459 (2013).
[4]W. Krieger, T. Suzuki, M. Völcker, and H. Walther, Phys. Rev. B **41**, 10229 (1990).
[5]M. Bttiker and R. Landauer, Phys. Scr. **32**, 429 (1985).
[6]M. J. Hagmann, Int. J. Quantum Chem. **56**, 289 (1995).
[7]P. K. Tien and J. P. Gordon, Phys. Rev. **129**, 647 (1963).
[8]A. J. Huber, F. Keilmann, J. Wittborn, J. Aizpurua, and R. Hillenbrand, Nano Lett. **8**, 3766 (2008).